

Genetic origins of the Minoans and Mycenaeans

Ioşif Lazaridis^{1,2*}, Alissa Mittnik^{3,4*}, Nick Patterson^{2,5}, Swapan Mallick^{1,2,6}, Nadin Rohland¹, Saskia Pfrengle⁴, Anja Furtwängler⁴, Alexander Peltzer^{3,7}, Cosimo Posth^{3,4}, Andonis Vasilakis⁸, P. J. P. McGeorge⁹, Eleni Konsolaki-Yannopoulou¹⁰, George Korres¹¹, Holley Martlew¹², Manolis Michalodimitrakis¹³, Mehmet Özsait¹⁴, Nesrin Özsait¹⁴, Anastasia Papanthanasidou¹⁵, Michael Richards¹⁶, Songül Alpaslan Roodenberg¹, Yannis Tzedakis¹⁷, Robert Arnott¹⁸, Daniel M. Fernandes^{19,20}, Jeffery R. Hughey²¹, Dimitra M. Lotakis²², Patrick A. Navas²², Yannis Maniatis²³, John A. Stamatoyannopoulos^{24,25,26}, Kristin Stewardson^{1,6}, Philipp Stockhammer^{3,27}, Ron Pinhasi^{19,28}, David Reich^{1,2,6}, Johannes Krause^{3,4} & George Stamatoyannopoulos^{22,25}

The origins of the Bronze Age Minoan and Mycenaean cultures have puzzled archaeologists for more than a century. We have assembled genome-wide data from 19 ancient individuals, including Minoans from Crete, Mycenaeans from mainland Greece, and their eastern neighbours from southwestern Anatolia. Here we show that Minoans and Mycenaeans were genetically similar, having at least three-quarters of their ancestry from the first Neolithic farmers of western Anatolia and the Aegean^{1,2}, and most of the remainder from ancient populations related to those of the Caucasus³ and Iran^{4,5}. However, the Mycenaeans differed from Minoans in deriving additional ancestry from an ultimate source related to the hunter-gatherers of eastern Europe and Siberia^{6–8}, introduced via a proximal source related to the inhabitants of either the Eurasian steppe^{1,6,9} or Armenia^{4,9}. Modern Greeks resemble the Mycenaeans, but with some additional dilution of the Early Neolithic ancestry. Our results support the idea of continuity but not isolation in the history of populations of the Aegean, before and after the time of its earliest civilizations.

Ancient DNA research has traced the principal ancestors of early European farmers to highly similar Neolithic populations of Greece and western Anatolia, beginning in the seventh millennium BC (refs 1, 2); however, the later history of these regions down to the Bronze Age, a transformational period in the history of Eurasia^{4,6,9}, is less clear. There is limited genetic evidence suggesting migrations from both the east (the area of Iran and the Caucasus), reaching Anatolia by at least ~3800 BC (ref. 4), and the north (eastern Europe and Siberia) contributing ‘Ancient North Eurasian’ ancestry^{6,10} to all modern Europeans. The timing and impact of these migrations in the Aegean is, however, unknown.

During the Bronze Age, two prominent archaeological cultures emerged in the Aegean. The culture of the island of Crete, sometimes referred to as ‘Minoan’¹¹, was Europe’s first literate civilization, and has been described as ‘Europe’s first major experience of civilization’¹². However, the Linear A syllabic ideographic and Cretan hieroglyphic scripts used by this culture remain undeciphered, obscuring its origins. Equally important was the civilization of the ‘Mycenaean’ culture of

mainland Greece, whose language, written in the Linear B script, was an early form of Greek¹³. Cretan influence in mainland Greece and the later Mycenaean occupation of Crete link these two archaeological cultures, but the degree of genetic affinity between mainland and Cretan populations is unknown. Greek is related to other Indo-European languages, leading to diverse theories tracing its earliest speakers from the seventh millennium down to ~1600 BC, and proposing varying degrees of population change (Supplementary Information section 1).

Genome-wide ancient DNA data provide a new source of information about the people of the Bronze Age, who were first known through the ancient poetic and historical traditions starting with Homer and Herodotus, later through the disciplines of archaeology and linguistics, and, more recently, by the limited information from ancient mitochondrial DNA^{14,15}. Here we answer several questions. First, do the labels ‘Minoan’ and ‘Mycenaean’ correspond to genetically coherent populations or do they obscure a more complex structure of the peoples who inhabited Crete and mainland Greece at this time? Second, how were the two groups related to each other, to their neighbours across the Aegean in Anatolia, and to other ancient populations from Europe^{1,2,6,8–10} and the Near East^{2–5,9,16,17}? Third, can inferences about their ancestral origins inform debates about the origins of their cultures? Fourth, how are the Minoans and Mycenaeans related to Modern Greeks, who inhabit the same area today?

We generated genome-wide data from 19 ancient individuals (Fig. 1a, Extended Data Table 1 and Supplementary Information section 1). These comprised ten Minoans from Crete (approximately 2900–1700 BC; labelled Minoan_Odigitria, from Moni Odigitria near the southern coast of central Crete; and Minoan_Lasithi, from the cave of Hagios Charalambos in the highland plain of Lasithi in east Crete). Four Mycenaeans were included from mainland Greece (approximately 1700–1200 BC; from the western coast of the Peloponnese, from Argolis, and the island of Salamis). An additional individual from Armenoi in western Crete (approximately 1370–1340 BC; labelled Crete_Armenoi) postdated the appearance of Mycenaean culture on the island. Our dataset also included a Neolithic sample from Alepotrypa Cave at Diros Bay in

¹Department of Genetics, Harvard Medical School, Boston, Massachusetts 02115, USA. ²Broad Institute of Harvard and MIT, Cambridge, Massachusetts 02142, USA. ³Max Planck Institute for the Science of Human History, 07745 Jena, Germany. ⁴Institute for Archaeological Sciences, University of Tübingen, 72074 Tübingen, Germany. ⁵Radcliffe Institute, Cambridge, Massachusetts 02138, USA. ⁶Howard Hughes Medical Institute, Harvard Medical School, Boston, Massachusetts 02115, USA. ⁷Integrative Transcriptomics, Centre for Bioinformatics, University of Tübingen, 72076 Tübingen, Germany. ⁸23rd Ephorate of Prehistoric and Classical Antiquities, 71202 Herakleion, Crete. ⁹British School at Athens, 106 76 Athens, Greece. ¹⁰26th Ephorate of Prehistoric and Classical Antiquities, Greek Ministry of Culture, 13536 Piraeus, Greece. ¹¹Department of Archaeology, University of Athens, 17584 Athens, Greece. ¹²The Holley Martlew Archaeological Foundation, The Hellenic Archaeological Foundation, Tivoli House, Tivoli Road, Cheltenham GL50 2TD, UK. ¹³University of Crete Medical School, 711 13 Herakleion, Crete, Greece. ¹⁴Erenköy, Bayar caddesi, Eser Apt. Number 7, Daire 24, Kadiköy, Istanbul, Turkey. ¹⁵Ephorate of Paleontology and Speleology, Greek Ministry of Culture, 11636 Athens, Greece. ¹⁶Department of Archaeology, Simon Fraser University, 8888 University Drive, Burnaby, British Columbia V5A 1S6, Canada. ¹⁷Hellenic Archaeological Service, Samara, 27, Paleo Psychico, 15452 Athens, Greece. ¹⁸Green Templeton College, University of Oxford, Woodstock Road, Oxford OX2 6HG, UK. ¹⁹School of Archaeology and Earth Institute, Belfield, University College Dublin, Dublin 4, Ireland. ²⁰CIAS, Department of Life Sciences, University of Coimbra, Coimbra 3000-456, Portugal. ²¹Division of Mathematics, Science, and Engineering, Hartnell College, 411 Central Avenue, Salinas, California 93901, USA. ²²Division of Medical Genetics, University of Washington, Seattle, Washington 98195, USA. ²³Laboratory of Archaeometry, National Center for Scientific Research ‘Demokritos’, Aghia Paraskevi 153 10, Attiki, Greece. ²⁴Department of Medicine, University of Washington, Seattle, Washington 98195, USA. ²⁵Department of Genome Sciences, University of Washington, Seattle, Washington 98195, USA. ²⁶Altius Institute for Biomedical Sciences, Seattle, Washington 98121, USA. ²⁷Ludwig-Maximilians-Universität München, Institut für Vor- und Frühgeschichtliche Archäologie und Provinzialrömische Archäologie, 80799 München, Germany. ²⁸Department of Anthropology, University of Vienna, Althanstraße 14, 1090 Vienna, Austria.

*These authors contributed equally to this work.

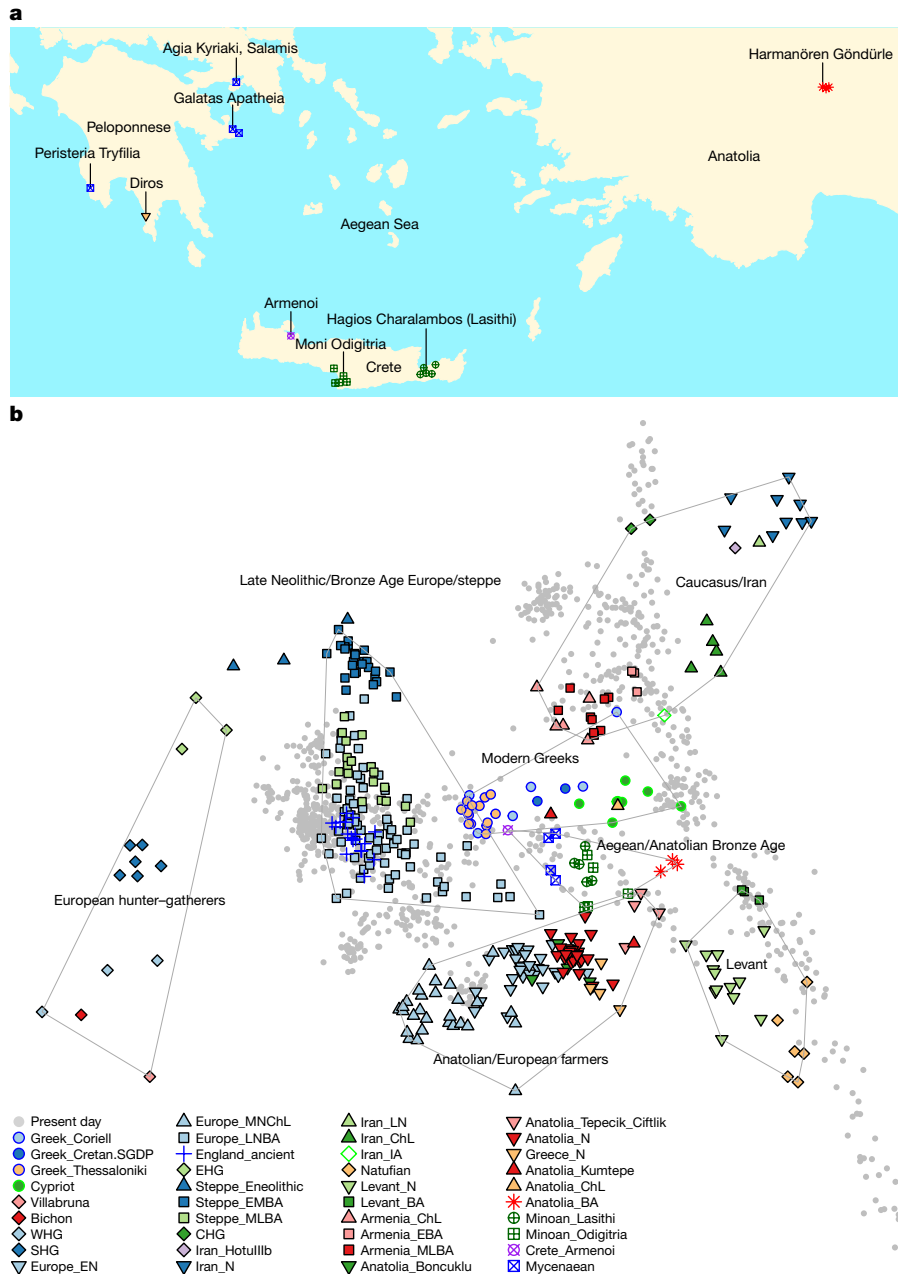


Figure 1 | Samples and PCA. **a**, Geographical locations of newly reported ancient data. Lines point to sampling locations; jitter is added to show the number of sampled individuals per location. **b**, Three hundred and thirty-four ancient individuals projected onto the first 2 principal

components computed on a sample of 1,029 present-day West Eurasians^{4,5,10,31}, including 30 Modern Greek samples from Greece and Cyprus. For abbreviations of population names, see Methods.

the southern Peloponnese (about 5400 BC), adding to previously published samples from northern Greece² (collectively labelled Greece_N). Finally, it included three Bronze Age individuals (approximately 2800–1800 BC; labelled Anatolia_BA) from Harmanören Gündürle in southwestern Anatolia (Turkey), adding knowledge about genetic variation in Anatolia after the Neolithic/Chalcolithic periods^{1,2,4,17} (Supplementary Information section 1). We processed the ancient remains, extracted DNA, and prepared Illumina libraries in dedicated clean rooms (Methods and Supplementary Table 1), and, after initial screening for mitochondrial DNA, used in-solution hybridization¹⁸ to capture ~1.2 million single nucleotide polymorphisms (SNPs)^{6,19} on the ancient samples. We assessed contamination by examining the rate at which they matched the mitochondrial consensus sequence (Supplementary Table 2) and the rate at which male samples were heterozygous on the X chromosome (Methods). We combined the dataset of the 19 ancient individuals with 332 other ancient

individuals from the literature, 2,614 present-day humans genotyped on the Human Origins array, and 2 present-day Cretans (Methods).

We performed principal component analysis (PCA)²⁰ (Methods), projecting ancient samples onto the first two principal components inferred from present-day West Eurasian populations¹⁰ that form two south–north parallel clines in Europe and the Near East along principal component 2. Minoans and Mycenaeans were centrally positioned in the PCA (Fig. 1b), framed to the left by ancient populations from mainland Europe and the Eurasian steppe, to the right by ancient populations from the Caucasus and Western Asia, and to the bottom by Early/Middle Neolithic farmers from Europe and Anatolia. The Neolithic samples from Greece clustered with these farmers and were distinct from the Minoans and Mycenaeans. The Bronze Age individuals from southwestern Anatolia were also distinct, intermediate between Anatolian and Levantine populations towards the bottom, and populations from Armenia, Iran, and the Caucasus

Table 1 | Admixture modelling of Bronze Age populations

Test	Ancestral sources				Mixture proportions				Standard errors			
	A	B	C	D	A	B	C	D	A	B	C	D
Ultimate sources	Anatolia_BA		CHG	Anatolia_N	Levant_N	0.319	0.618	0.063		0.029	0.078	0.063
	Minoan_Odigitria		CHG	Anatolia_N		0.144	0.856			0.031	0.031	
	Minoan_Odigitria		Iran_N	Anatolia_N		0.137	0.863			0.032	0.032	
	Minoan_Lasithi	MA1	CHG	Anatolia_N		0.001	0.152	0.847		0.015	0.021	0.020
	Minoan_Lasithi	Mota	CHG	Anatolia_N		0.004	0.154	0.842		0.024	0.026	0.020
	Mycenaean	AfontovaGora3	CHG	Anatolia_N		0.133	0.126	0.741		0.027	0.026	0.024
	Mycenaean	AfontovaGora3	Iran_N	Anatolia_N		0.161	0.086	0.754		0.026	0.025	0.024
	Mycenaean	EHG	Iran_N	Anatolia_N		0.065	0.136	0.799		0.016	0.022	0.024
	Mycenaean	EHG	CHG	Anatolia_N		0.044	0.176	0.780		0.016	0.023	0.024
	Mycenaean	MA1	CHG	Anatolia_N		0.052	0.159	0.789		0.019	0.026	0.024
Proximate sources	Anatolia_BA		Anatolia_ChL	Natufian		0.908	0.092			0.039	0.039	
	Anatolia_BA		Anatolia_ChL	Levant_BA		0.892	0.108			0.114	0.114	
	Anatolia_BA		Anatolia_ChL	Levant_N		0.951	0.049			0.051	0.051	
	Anatolia_BA		Anatolia_ChL	Anatolia_N			0.935	0.065			0.062	0.062
	Mycenaean		Armenia_MLBA	Anatolia_N		0.367	0.633			0.020	0.020	
	Mycenaean		Armenia_ChL	Anatolia_N		0.441	0.559			0.025	0.025	
	Anatolia_BA		Anatolia_ChL	Minoan_Lasithi		0.970	0.030			0.108	0.108	
	Mycenaean	Steppe_MLBA		Minoan_Lasithi		0.175	0.825			0.017	0.017	
	Mycenaean	Europe_LNBA		Minoan_Lasithi		0.198	0.802			0.019	0.019	
	Mycenaean	Steppe_EMBA		Minoan_Lasithi		0.132	0.868			0.014	0.014	

For each test population, mixture proportions from four source populations with their standard errors are given. Ancestry is inferred from both 'ultimate' sources representing the earliest populations, and 'proximate' sources representing populations down to the Bronze Age (Supplementary Information section 2). Column A lists 'northern' sources from eastern Europe and Siberia, including the Eurasian steppe; column B lists 'eastern' sources from Iran, the Caucasus, and Anatolia (after the Early Neolithic); column C lists 'local' sources from Anatolia and the Aegean; column D lists sources from the Levant. For abbreviations of population names, see Methods.

towards the top. ADMIXTURE analysis (Methods and Extended Data Fig. 1) showed that Minoans and Mycenaeans both possessed a 'pink' genetic component ($K = 8$ and greater) shared with Bronze Age southwestern Anatolians, Neolithic Central Anatolians from Tepecik-Çiftlik¹⁷, a Chalcolithic northwestern Anatolian¹, and western Anatolians from Kumtepe¹⁶. This component was maximized in the Mesolithic/Neolithic samples from Iran^{4,5} and hunter-gatherers from the Caucasus³ (Extended Data Fig. 1). It was not found in the Neolithic of northwestern Anatolia, Greece, or the Early/Middle Neolithic populations of the rest of Europe, only appearing in the populations of the Late Neolithic/Bronze Age in mainland Europe⁶, introduced there by migration from the Eurasian steppe¹⁶.

Beyond the visual impressions of PCA and ADMIXTURE, we formally tested the relationships among populations from our study and the literature, using f_4 -statistics of the form $f_4(X, Y; \text{Test}, \text{Chimp})$ that evaluated whether Test shared more alleles with X or Y. We found that Test populations from Iran, the Caucasus, and eastern Europe shared more alleles with Minoans and Mycenaeans than with the Neolithic population of Greece (Extended Data Fig. 2a, b). The Minoans from the Lasithi plateau in the highlands of eastern Crete and from the coast of southern Crete (Extended Data Fig. 2c) were consistent with being a homogeneous population. Mycenaeans differed from these Minoans in sharing significantly fewer alleles with Neolithic people from the Levant, Anatolia, Greece, and mainland Europe (Extended Data Fig. 2d). In comparison, the Bronze Age Anatolians shared fewer alleles with ancient Europeans and more with ancient populations of Iran and the Levant (Extended Data Fig. 3). We used f_3 -statistics of the form $f_3(\text{Ref}_1, \text{Ref}_2; \text{Test})$ that, if negative, showed that Test was admixed from sources related to the $\text{Ref}_1, \text{Ref}_2$ source populations. We did not find significantly negative ($\text{Ref}_1, \text{Ref}_2$) pairs for Minoans or Bronze Age Anatolians ($z > -2.5$), but did for Mycenaeans ($-4.9 < z < -3.0$; Extended Data Fig. 4), involving early farmers from the Levant, Anatolia, Greece, and the rest of Europe as one source, and Iran or the Eurasian steppe or steppe-influenced Europeans as the other.

We modelled Bronze Age populations using the qpAdm/qpWave⁶ framework (Methods and Supplementary Information section 2), which relates a set of 'left' populations (admixed population and ancestral source populations) with a set of 'right' populations (diverse outgroups) and allows testing for the number of streams of ancestry from 'right' to 'left' and estimation of admixture proportions. This analysis showed that all Bronze Age populations from the Aegean and

Anatolia are consistent with deriving most (approximately 62–86%) of their ancestry from an Anatolian Neolithic-related population (Table 1). However, they also had a component (approximately 9–32%) of 'eastern' (Caucasus/Iran-related) ancestry. It was previously shown that this type of ancestry was introduced into mainland Europe via Bronze Age pastoralists from the Eurasian steppe, who were a mix of both eastern European hunter-gatherers and populations from the Caucasus and Iran^{4,6}; our results show that it also arrived on its own, at least in the Minoans, without eastern European hunter-gatherer ancestry. This ancestry need not have arrived from regions east of Anatolia, as it was already present during the Neolithic in central Anatolia at Tepecik-Çiftlik¹⁷ (Supplementary Information section 2). The eastern influence in the Bronze Age populations from Greece and southwestern Anatolia is also supported by an analysis of their Y chromosomes. Four out of five males belonging to Minoans, Mycenaeans, and southwestern Anatolians (Supplementary Information section 3) belonged to haplogroup J, which was rare or non-existent in earlier populations from Greece and western Anatolia who were dominated by Y-chromosome haplogroup G2 (refs 1, 2, 17). Haplogroup J was present in Caucasus hunter-gatherers³ and a Mesolithic individual from Iran⁴, and its spread westwards may have accompanied the 'eastern' genome-wide influence.

The Minoans could be modelled as a mixture of the Anatolia Neolithic-related substratum with additional 'eastern' ancestry, but the other two groups had additional ancestry: the Mycenaeans had approximately 4–16% ancestry from a 'northern' ultimate source related to the hunter-gatherers of eastern Europe and Siberia (Table 1), while the Bronze Age southwestern Anatolians may have had ~6% ancestry related to Neolithic Levantine populations. The elite Mycenaean individual from the 'royal' tomb at Peristeria in the western Peloponnese did not differ genetically from the other three Mycenaean individuals buried in common graves. To identify more proximate sources of the distinctive eastern European/north Eurasian-related ancestry in Mycenaeans, we included later populations as candidate sources (Supplementary Information section 2), and could model Mycenaeans as a mixture of the Anatolian Neolithic and Chalcolithic-to-Bronze Age populations from Armenia (Table 1). Populations from Armenia possessed some ancestry related to eastern European hunter-gatherers⁴, so they, or similar unsampled populations of western Asia, could have contributed it to populations of the Aegean. This model makes geographical sense, since a population movement from the vicinity of

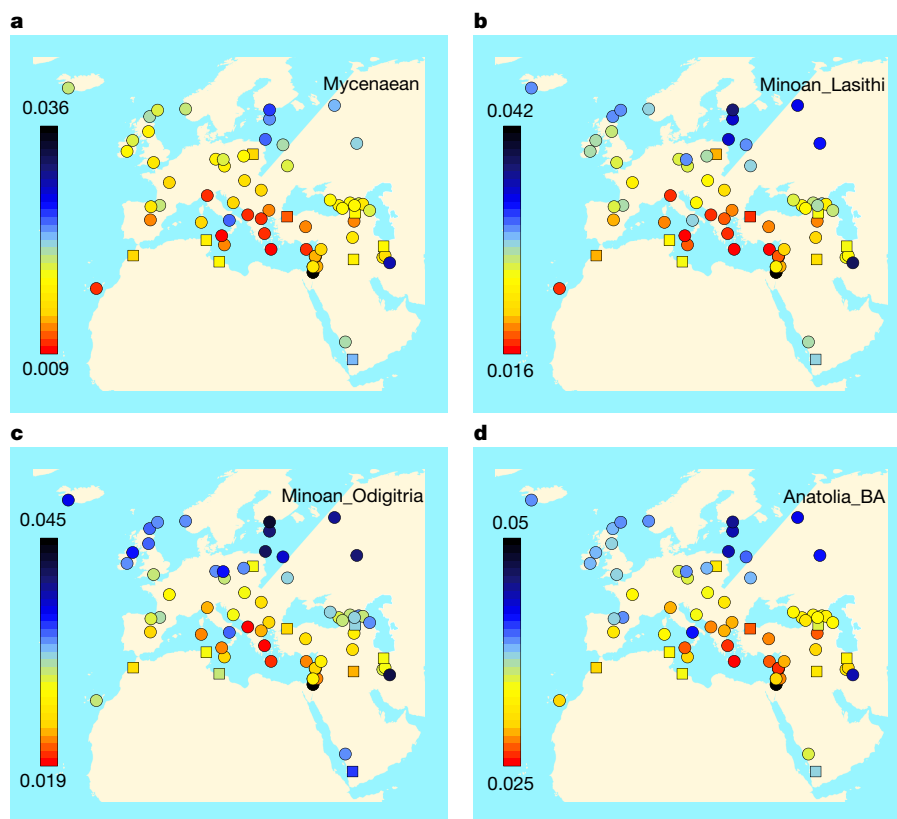


Figure 2 | Genetic differentiation of Bronze Age populations to present-day populations. The F_{ST} inbreeding coefficient (Methods) between newly reported populations and present-day West Eurasian populations. This shows a pattern of genetic affinity between Bronze Age and present-day populations from the corresponding broad

geographical regions: **a**, Mycenaean; **b**, Minoans from Hagios Charalambos (Lasithi regional unit); **c**, Minoans from Moni Odigitria (Herakleion regional unit); **d**, southwestern Bronze Age (BA) Anatolians. The same pattern also applies to Bronze Age populations from other regions of West Eurasia (Extended Data Fig. 5).

Armenia could have admixed with Anatolian Neolithic-related farmers on either side of the Aegean. However, Mycenaeans can also be modelled as a mixture of Minoans and Bronze Age steppe populations (Table 1 and Supplementary Information section 2), suggesting that, alternatively, ‘eastern’ ancestry arrived in both Crete and mainland Greece, followed by about 13–18% admixture with a ‘northern’ steppe population in mainland Greece only. Such a scenario is also plausible: first, it provides a genetic correlate for the distribution of shared toponyms in Crete, mainland Greece, and Anatolia discovered in ref. 21; second, it postulates a single migration from the east; third, it proposes some gene flow from geographically contiguous areas to the north where steppe ancestry was present since at least the mid-third millennium BC (refs 6, 9). We validated inferences from qpAdm by treating source populations as ‘ghosts’ and re-estimating mixture proportions⁴, by examining the correspondence between qpAdm estimates and PCA⁴ (Extended Data Fig. 5), and by comparing simulated individuals of known ancestry against the Mycenaeans (Extended Data Fig. 6).

Geographical structure may have prevented the spread of the ‘northern’ ancestry from the mainland to Crete, contributing to genetic differentiation. Such a structure may, in principle, be long-standing, even before the advent of the Neolithic in the seventh millennium BC. Alternatively, both ‘northern’ and ‘eastern’ ancestry may have arrived in the Aegean at any time between the Early Neolithic and the Late Bronze Age. Wider geographical and temporal sampling of pre-Bronze Age populations of the Aegean may better trace the advent of ‘northern’ and ‘eastern’ ancestry in the region. However, sampled Neolithic samples from Greece, down to the Final Neolithic ~4100 BC (ref. 2), do not possess either type of ancestry, suggesting that the admixture we detect probably occurred during the fourth to second millennium BC time window. Other proposed migrations, such as settlement by Egyptian or Phoenician colonists²², are not discernible

in our data, as there is no measurable Levantine or African influence in the Minoans and Mycenaeans, thus rejecting the hypothesis that the cultures of the Aegean were seeded by migrants from the old civilizations of these regions. On the other hand, migrants from areas east or north of the Aegean, while numerically less influential than the locals, may have contributed to the emergence of the third to second millennium BC Bronze Age cultures as ‘creative disruptors’ of local traditions, bearers of innovations, or through cultural interaction with the locals, coinciding with the genetic process of admixture²³. Relative ancestral contributions do not determine the relative roles in the rise of civilization of the different ancestral populations; nonetheless, the strong persistence of the Neolithic substratum does suggest a key role for the locals in this process.

Phenotype prediction from genetic data has enabled the reconstruction of the appearance of ancient Europeans^{1,24} who left no visual record of their pigmentation. By contrast, the appearance of the Bronze Age people of the Aegean has been preserved in colourful frescos and pottery, depicting people with mostly dark hair and eyes²⁵. We used the HirisPlex²⁶ tool (Supplementary Information section 4) to infer that the appearance of our ancient samples matched the visual representations (Extended Data Table 2), suggesting that art of this period reproduced phenotypes naturalistically.

We estimated the fixation index, F_{ST} , of Bronze Age populations with present-day West Eurasians, finding that Mycenaeans were least differentiated from populations from Greece, Cyprus, Albania, and Italy (Fig. 2), part of a general pattern in which Bronze Age populations broadly resembled present-day inhabitants from the same region (Extended Data Fig. 7). Modern Greeks occupy the intermediate space of the PCA along principal component 1 (Fig. 1b) between ancient European and Near Eastern populations, such as those of the Bronze Age. They are not, however, identical to Bronze Age populations, as

they are above them along principal component 2 (Fig. 1b). This is because Neolithic farmers shared fewer alleles with Modern Greeks than with Mycenaean (Extended Data Fig. 8), consistent with additional later admixture^{27,28}.

The Minoans and Mycenaean, sampled from different sites in Crete and mainland Greece, were homogeneous, supporting the genetic coherency of these two groups. Differences between them were modest, viewed against their broad overall similarity to each other and to the southwestern Anatolians, sharing in both the 'local' Anatolian Neolithic-like farmer ancestry and the 'eastern' Caucasus-related admixture. Two key questions remain to be addressed by future studies. First, when did the common 'eastern' ancestry of both Minoans and Mycenaean arrive in the Aegean? Second, is the 'northern' ancestry in Mycenaean due to sporadic infiltration of Greece, or to a rapid migration as in Central Europe⁶? Such a migration would support the idea that proto-Greek speakers²⁹ formed the southern wing of a steppe intrusion of Indo-European speakers. Yet, the absence of 'northern' ancestry in the Bronze Age samples from Pisidia, where Indo-European languages were attested in antiquity, casts doubt on this genetic-linguistic association, with further sampling of ancient Anatolian speakers needed. Whatever the answer to these questions, the discovery of at least two migration events into the Aegean in addition to the first farming dispersal before the Bronze Age, and of additional population change since that time, supports the view that the Greeks did not emerge fully formed from the depths of prehistory, but were, indeed, a people 'ever in the process of becoming'³⁰.

Online Content Methods, along with any additional Extended Data display items and Source Data, are available in the online version of the paper; references unique to these sections appear only in the online paper.

Received 21 December 2016; accepted 25 June 2017.

Published online 2 August 2017.

- Mathieson, I. *et al.* Genome-wide patterns of selection in 230 ancient Eurasians. *Nature* **528**, 499–503 (2015).
- Hofmanová, Z. *et al.* Early farmers from across Europe directly descended from Neolithic Aegeans. *Proc. Natl Acad. Sci. USA* **113**, 6886–6891 (2016).
- Jones, E. R. *et al.* Upper Palaeolithic genomes reveal deep roots of modern Eurasians. *Nat. Commun.* **6**, 8912 (2015).
- Lazaridis, I. *et al.* Genomic insights into the origin of farming in the ancient Near East. *Nature* **536**, 419–424 (2016).
- Broushaki, F. *et al.* Early Neolithic genomes from the eastern Fertile Crescent. *Science* **353**, 499–503 (2016).
- Haak, W. *et al.* Massive migration from the steppe was a source for Indo-European languages in Europe. *Nature* **522**, 207–211 (2015).
- Raghavan, M. *et al.* Upper Palaeolithic Siberian genome reveals dual ancestry of Native Americans. *Nature* **505**, 87–91 (2014).
- Fu, Q. *et al.* The genetic history of Ice Age Europe. *Nature* **534**, 200–205 (2016).
- Allentoft, M. E. *et al.* Population genomics of Bronze Age Eurasia. *Nature* **522**, 167–172 (2015).
- Lazaridis, I. *et al.* Ancient human genomes suggest three ancestral populations for present-day Europeans. *Nature* **513**, 409–413 (2014).
- Evans, A. *The Palace of Minos; a Comparative Account of the Successive Stages of the Early Cretan Civilization as Illustrated by the Discoveries at Knossos* (Macmillan, 1921).
- Willets, R. F. *The Civilization of Ancient Crete* (Univ. California Press, 1992).
- Chadwick, J. *The Decipherment of Linear B* 2nd edn (Cambridge Univ. Press, 1967).
- Hughey, J. R. *et al.* A European population in Minoan Bronze Age Crete. *Nat. Commun.* **4**, 1861 (2013).
- Bouwman, A. S., Brown, K. A., Prag, A. J. N. W. & Brown, T. A. Kinship between burials from Grave Circle B at Mycenae revealed by ancient DNA typing. *J. Archaeol. Sci.* **35**, 2580–2584 (2008).
- Omrak, A. *et al.* Genomic evidence establishes Anatolia as the source of the European Neolithic gene pool. *Curr. Biol.* **26**, 270–275 (2016).
- Kilinc, G. M. *et al.* The demographic development of the first farmers in Anatolia. *Curr. Biol.* **26**, 2659–2666 (2016).
- Fu, Q. *et al.* DNA analysis of an early modern human from Tianyuan Cave, China. *Proc. Natl Acad. Sci. USA* **110**, 2223–2227 (2013).
- Fu, Q. *et al.* An early modern human from Romania with a recent Neanderthal ancestor. *Nature* **524**, 216–219 (2015).
- Patterson, N., Price, A. L. & Reich, D. Population structure and eigenanalysis. *PLoS Genet.* **2**, e190 (2006).
- Kretschmer, P. *Einleitung in die Geschichte der griechischen Sprache* (Vandenhoeck und Ruprecht, 1896).
- Bernal, M. *Black Athena: The Afroasiatic Roots of Classical Civilization (The Fabrication of Ancient Greece 1785–1985, Volume 1)* (Rutgers Univ. Press, 1987).
- Angel, J. L. Social biology of Greek culture growth. *Am. Anthropol.* **48**, 493–533 (1946).
- Wilde, S. *et al.* Direct evidence for positive selection of skin, hair, and eye pigmentation in Europeans during the last 5,000 y. *Proc. Natl Acad. Sci. USA* **111**, 4832–4837 (2014).
- Dickinson, O. *The Aegean Bronze Age* (Cambridge Univ. Press, 1994).
- Walsh, S. *et al.* The HirisPlex system for simultaneous prediction of hair and eye colour from DNA. *Forensic Sci. Int. Genet.* **7**, 98–115 (2013).
- Hellenthal, G. *et al.* A genetic atlas of human admixture history. *Science* **343**, 747–751 (2014).
- Ralph, P. & Coop, G. The geography of recent genetic ancestry across Europe. *PLoS Biol.* **11**, e1001555 (2013).
- Sakellariou, M. B. *Les Proto-grecs (Le peuplement de la Grèce et du bassin Egéen aux hautes époques)* (Ekdotike Athenon, 1980).
- Myres, J. L. *Who were the Greeks?* (Univ. California Press, 1930).
- Patterson, N. *et al.* Ancient admixture in human history. *Genetics* **192**, 1065–1093 (2012).

Supplementary Information is available in the online version of the paper.

Acknowledgements We thank M. McCormick for comments and critiques, F. Göhringer, I. Kucukkalipci, and G. Brandt for wet laboratory support, and S. Pääbo for providing access to the clean room facilities at the MPI-EVA, Leipzig. We thank the Hellenic Ministry of Culture, the Hellenic Archaeological Service, and the Turkish Ministry of Culture and Tourism for approval of our studies, and the personnel of the Hagios Nikolaos, Herakleion, Pireas, Olympia, Chora (Trifylia), and Sparta Museums for facilitating sample collection. All maps were plotted in R using the worldHiRes map of the 'mapdata' package (using data in the public domain from the CIA World Data Bank II). Research on Hagios Charalambos cave by P.J.P.McG. was supported by the Royal Society and the Institute for Aegean Prehistory (INSTAP). D.M.F. was supported by an Irish Research Council grant (GOIPG/2013/36). J.K. and A.M. were funded by Deutsche Forschungsgemeinschaft grant KR 4015/1-1 and the Max Planck Society. D.R. was supported by National Institutes of Health grant GM100233, by National Science Foundation HOMINID BCS-1032255, and is a Howard Hughes Medical Institute investigator. The study of the ancient Minoans and Mycenaean was supported by the Lucile P. Markey Charitable Trust to G.S.

Author Contributions G.S. conceived the study. D.R. and J.K. co-supervised the ancient DNA work, sequencing, and data analysis. I.L. performed population genetics analysis and wrote the manuscript with input from other authors. P.J.P.McG., E.K.-Y., G.K., H.M., M.M., M.O., N.O., A.Pa., M.R., S.A.R., Y.T., A.V., R.A., P.S., R.P., J.K., and G.S. assembled, studied, or described archaeological and osteological material. A.M., S.P., N.R., A.F., C.P., D.M.F., J.R.H., D.M.L., Y.M., J.A.S., K.St., R.P., G.S., D.R., P.A.N., and J.K. performed wet laboratory work. A.M., N.P., S.M., and A.Pe., performed bioinformatics analyses.

Author Information Reprints and permissions information is available at www.nature.com/reprints. The authors declare no competing financial interests. Readers are welcome to comment on the online version of the paper. Publisher's note: Springer Nature remains neutral with regard to jurisdictional claims in published maps and institutional affiliations. Correspondence and requests for materials should be addressed to I.L. (lazaridis@genetics.med.harvard.edu), D.R. (reich@genetics.med.harvard.edu), J.K. (krause@shh.mpg.de), or G.S. (gstam@u.washington.edu).

Reviewer Information Nature thanks R. Nielsen, C. Renfrew, B. Shapiro and the other anonymous reviewer(s) for their contribution to the peer review of this work.

METHODS

No statistical methods were used to predetermine sample size. The experiments were not randomized and the investigators were not blinded to allocation during experiments and outcome assessment.

Ancient DNA. An overview of which steps in processing the ancient samples were undertaken in which laboratory is provided in Supplementary Table 1.

Dublin, Ireland. The inner ear area of each petrous bone was identified, isolated, then ground to a fine powder. Cleaning and isolation of the cochlea was performed using aluminium oxide powder in a sandblasting chamber. Once isolated, it was decontaminated by ultraviolet irradiation for 7.5 min on each side, ground on a mixer mill to a weight of about 50 mg, and finally transferred to a sterile Eppendorf tube. All procedures were conducted in clean and dedicated ancient DNA facilities.

Seattle, Washington, USA. Teeth processed in this laboratory were decontaminated and pulverized to powder in clean and dedicated ancient DNA facilities following previously published methods¹¹.

Leipzig, Germany. As previously described³², sampling, extraction, and preparation of double-indexed, double-stranded libraries took place in the clean room facilities of the Max Planck Institute for Evolutionary Anthropology, Leipzig, Germany (MPI-EVA), followed by enrichment of human mitochondrial DNA³³. Enriched libraries were sequenced on an Illumina GAIIx platform for $2 \times 76 + 7$ cycles and the resulting data were mapped to the revised Cambridge Reference Sequence using the EAGER pipeline to evaluate DNA preservation (Supplementary Table 2). These libraries were then shipped to Boston, Massachusetts, USA, where nuclear target enrichment was performed (see below).

Tübingen, Germany. Pre-PCR steps took place in the clean room facilities of the Institute for Archaeological Sciences at the University of Tübingen, Germany. After surface irradiation with ultraviolet light, the tooth was sawn apart transversally at the border of crown and root, and dentine powder from the inside the crown was sampled using a sterile dentistry drill. Extraction, library preparation, and enrichment of human mitochondrial DNA used the same protocols as described for MPI-EVA, with the addition of an updated extraction protocol³⁴. Sequencing of shotgun and mitochondrial-DNA-enriched libraries took place at the facilities of the Frauenklinik of the University of Tübingen, on an Illumina MiSeq for $2 \times 150 + 8$ cycles or on an Illumina HiSeq 2500 for $2 \times 101 + 8$ cycles (Supplementary Table 2).

Additional libraries were produced including full or partial³⁵ repair with uracil-DNA glycosylase and endonuclease VIII to remove deaminated bases. In-solution enrichment was performed using previously reported protocols^{6,18}. Two SNP sets of 394,577 SNPs (‘390k capture’⁶) or 1,237,207 SNPs (‘1240k capture’¹¹) were targeted. Sequencing took place in the facilities of the Frauenklinik, University of Tübingen, on an Illumina HiSeq 2500 for $2 \times 101 + 8$ cycles and at the facilities of the University of Kiel on a HiSeq 4000 for $2 \times 150 + 8$ cycles. One uracil-DNA glycosylase-treated library (I0071) was sent to Boston, Massachusetts, for nuclear target enrichment (see below).

Boston, Massachusetts, USA. The bone powders, prepared from petrous bones in Dublin, Ireland, were sent to Boston, where DNA extractions and barcoded library preparations without uracil removal were performed in the Harvard Medical School cleanroom following previously described protocols^{34–36}. At the screening stage, libraries were (1) shotgun sequenced and (2) sequenced after enriching for the human mitochondrial DNA³⁷ together with some nuclear loci to approximate the nuclear coverage and mitochondrial contamination.

All four libraries (barcoded) prepared in Boston, three libraries (indexed) prepared in Leipzig, and one library (indexed) prepared in Tübingen, were used to perform 390k (ref. 6) and 840k (ref. 19) or 1240k (=390k + 840k) targeted capture of a total of 1,233,013 SNPs, following the in-solution target enrichment protocol in ref. 18 and sequenced either on an Illumina HiSeq 2500 or an Illumina NextSeq 500 (see Supplementary Table 1 for details).

For each sample, each SNP position was represented by a randomly chosen sequence, restricting to those with a minimum mapping quality (MAPQ ≥ 10), sites with a minimum sequence quality (≥ 20), and removing two bases at the ends of reads⁴.

Testing for contamination. Modern human contamination of the mitochondrial DNA was assessed using the software *schmutzi*³⁸, which took into account that the consensus sequence should be reconstructed from reads showing characteristics of ancient DNA and originating from a single individual (Supplementary Table 2). We assessed contamination by examining heterozygosity on the X chromosome in five males (possessing only one copy of the X chromosome) using ANGSD³⁹ (Supplementary Information section 3); this was in the range 0.3–4%. Indirect evidence that the females in our dataset (for which X-chromosome-based contamination estimation was impossible) were authentic was furnished by their clustering with male samples and distinctiveness from present-day Greek or central European populations that may have possibly contaminated them (Fig. 1b). We also

computed f_4 -statistics of the form $f_4(\text{Males, Females; Test, Chimp})$ for populations that had both male and female individuals for all ancient or present-day Test populations in our dataset. If female samples were substantially contaminated from a source related to Test, these statistics would be significantly negative; however, we found that the Z-score of these statistics was $-1.6 < Z < 2.5$. We thus included both male and female samples in our analysis to maximize sample size instead of restricting it to damaged molecules for females⁸.

Modern human data. We used a dataset of 2,614 individuals genotyped on the Affymetrix Human Origins array^{4,5,10,31}, including 28 Modern Greek (from Greece and Cyprus) samples previously described¹⁰. We also included data from two Modern Greeks from Crete whose whole-genome sequences were published as part of the Simons Genome Diversity Project⁴⁰. We also analysed Modern Greek data from Thessaly and Central Greece⁴¹ and diverse regions^{27,42} genotyped on Illumina arrays.

Datasets. We analysed two datasets: HO, which includes the Affymetrix Human Origins genotyping data together with 351 ancient humans (including samples from the literature^{1–5,7–10,16,17,43–51} and the newly reported data) on 591,642 autosomal SNPs; and the HOIII dataset, which does not include the Human Origins data, but has a larger number of 1,054,671 autosomal SNPs⁴. We did not use previously performed genotype calls of data from the literature, but re-processed them, beginning with the original data release format (FASTQ or BAM). The main analysis dataset was HOIII, except for analyses that included modern populations, in which case the HO dataset was analysed. For the analysis of Illumina genotype data of Modern Greeks (Extended Data Fig. 6), a total of 489,148 autosomal SNPs were analysed.

Abbreviations used. For brevity, we used the following abbreviations in population names, following the convention of ref. 4: CHG, Caucasus hunter-gatherers; EHG, Eastern European hunter-gatherers; WHG, Western European hunter-gatherers; SHG, Scandinavian hunter-gatherers; N, Neolithic; EN, Early Neolithic; MN, Middle Neolithic; ChL, Chalcolithic; LNBA, Late Neolithic/Bronze Age; BA, Bronze Age; EBA, Early Bronze Age; EMBA, Early/Middle Bronze Age; MLBA, Middle/Late Bronze Age; IA, Iron Age.

PCA. PCA was performed in the smartpca program of EIGENSOFT²⁰, using default parameters and the *lsproject*: YES¹⁰ and *numoutlieriter*: 0 options. PCA was performed on 1,029 present-day West Eurasians and 334 ancient samples were projected (Fig. 1b); Upper Palaeolithic individuals before the appearance of the Villabruna cluster⁸ plot in the middle of present-day West Eurasian variation and are not shown.

ADMIXTURE analysis. ADMIXTURE analysis⁵² of the HO dataset was performed after pruning for linkage disequilibrium in PLINK^{53,54} with parameters *indep-pairwise* 200 25 0.4, after which 299,971 SNPs were retained. Twenty replicates of the analysis were performed with different random seeds, and the highest likelihood replicate for each value of K was retained. We show the $K = 2$ to $K = 17$ results for the 351 ancient and 30 Modern Greek samples in Extended Data Fig. 1.

f -statistics. The f_3 - and f_4 -statistics were computed in ADMIXTOOLS³¹ using the programs *qp3Pop* and *qpF4ratio* with default parameters, and *qpDstat* with *f4mode*: YES. Standard errors were computed with a block jack-knife⁵⁵. When an ancient population was the target for f_3 -statistics, we set the *inbreed*: YES parameter, as our data were represented by pseudo-haploid genotypes, which introduced artificial genetic drift that masked the negative signal of admixture³¹.

Testing for the number of streams of ancestry and estimating mixture proportions. We used the *qpWave*^{6,56,57}/*qpAdm*⁶ framework, which relates a set of ‘left’ populations (the population of interest and candidate ancestral sources) to a set of ‘right’ populations (diverse outgroups), testing for the number of streams of ancestry from ‘right’ to ‘left’ and estimating mixture proportions.

Simulations of admixed individuals. We simulated admixed individuals (Supplementary Information section 2) given a set of sources and mixture proportions by first sampling (at each SNP) one of the sources (according to the mixture proportions), and then one of the individuals from that population (with equal probability). Because of missingness, the data-generating mixture proportions did not correspond precisely to the actual ancestry of simulated individuals and we corrected for this bias (Supplementary Information section 2). We noted the maximum absolute value of the Z-score of the statistic $f_4(\text{Mycenaean, Simulated; A, B})$, where A, B were two outgroup populations to test whether, for a particular choice of ancestry of Simulated, it formed a clade with the sampled Mycenaeans.

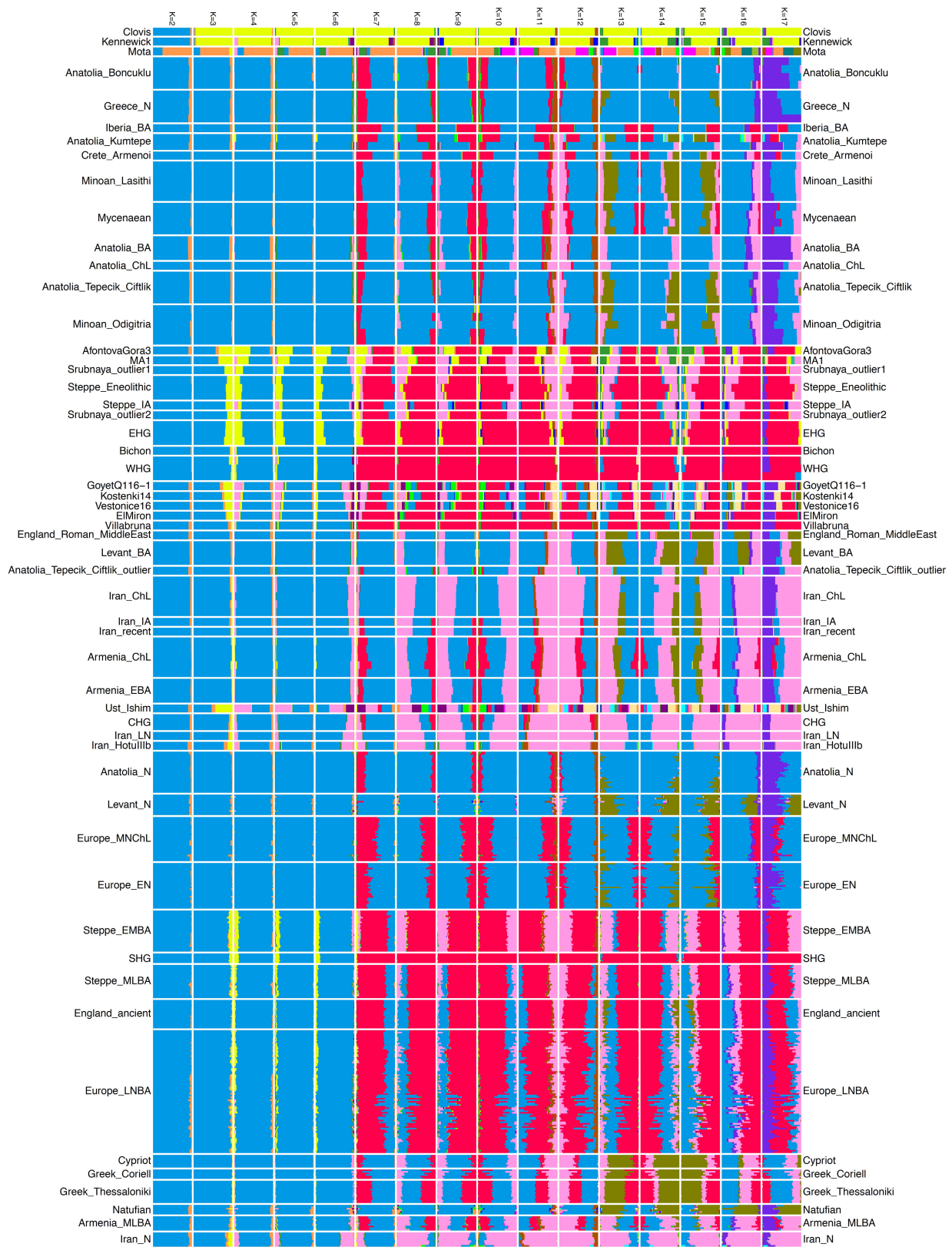
Estimation of F_{ST} coefficients. We estimated F_{ST} in *smartpca*²⁰ with the default parameters *inbreed*: YES⁵⁷, and *fstonly*: YES.

Phenotypic inference. The ancient samples had low coverage (median $0.87 \times$) and thus diploid genotypes could not be reliably assessed for them. However, we could use the low coverage data to compute allele frequencies in all individuals and the Bronze Age Aegean using a likelihood approach¹. We then sampled from the posterior distribution of the genotypes g given the read counts r of the reference allele and t of the total reads covering a site. We took 100 random genotype samples

per individuals and submitted them to HIRISplex²⁶, obtaining an estimate of the uncertainty of phenotype inference (Supplementary Information section 4 and Extended Data Table 2).

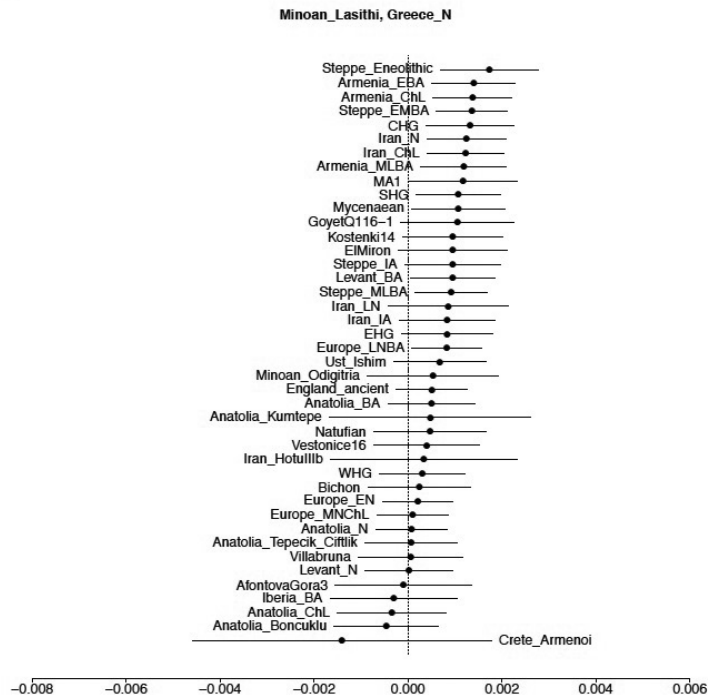
Data availability. The aligned sequences are available through the European Nucleotide Archive under accession number PRJEB20914. Genotype datasets used in analysis are available at <https://reich.hms.harvard.edu/datasets>. All other data are available from the corresponding authors upon reasonable request.

32. Fu, Q. *et al.* A revised timescale for human evolution based on ancient mitochondrial genomes. *Curr. Biol.* **23**, 553–559 (2013).
33. Maricic, T., Whitten, M. & Pääbo, S. Multiplexed DNA sequence capture of mitochondrial genomes using PCR products. *PLoS ONE* **5**, e14004 (2010).
34. Dabney, J. *et al.* Complete mitochondrial genome sequence of a Middle Pleistocene cave bear reconstructed from ultrashort DNA fragments. *Proc. Natl Acad. Sci. USA* **110**, 15758–15763 (2013).
35. Rohland, N., Harney, E., Mallick, S., Nordenfelt, S. & Reich, D. Partial uracil–DNA–glycosylase treatment for screening of ancient DNA. *Phil. Trans. R. Soc. B* **370**, 20130624 (2015).
36. Korlević, P. *et al.* Reducing microbial and human contamination in DNA extractions from ancient bones and teeth. *Biotechniques* **59**, 87–93 (2015).
37. Meyer, M. *et al.* A mitochondrial genome sequence of a hominin from Sima de los Huesos. *Nature* **505**, 403–406 (2014).
38. Renaud, G., Slon, V., Duggan, A. T. & Kelso, J. Schmutzi: estimation of contamination and endogenous mitochondrial consensus calling for ancient DNA. *Genome Biol.* **16**, 224 (2015).
39. Korneliussen, T. S., Albrechtsen, A. & Nielsen, R. ANGSD: Analysis of Next Generation Sequencing Data. *BMC Bioinformatics* **15**, 356 (2014).
40. Mallick, S. *et al.* The Simons Genome Diversity Project: 300 genomes from 142 diverse populations. *Nature* **538**, 201–206 (2016).
41. Behar, D. M. *et al.* No evidence from genome-wide data of a Khazar origin for the Ashkenazi Jews. *Hum. Biol.* **85**, 859–900 (2013).
42. Busby, G. B. J. *et al.* The role of recent admixture in forming the contemporary West Eurasian genomic landscape. *Curr. Biol.* **25**, 2518–2526 (2015).
43. Cassidy, L. M. *et al.* Neolithic and Bronze Age migration to Ireland and establishment of the insular Atlantic genome. *Proc. Natl Acad. Sci. USA* **113**, 368–373 (2016).
44. Fu, Q. *et al.* Genome sequence of a 45,000-year-old modern human from western Siberia. *Nature* **514**, 445–449 (2014).
45. Günther, T. *et al.* Ancient genomes link early farmers from Atapuerca in Spain to modern-day Basques. *Proc. Natl Acad. Sci. USA* **112**, 11917–11922 (2015).
46. Llorente, M. G. *et al.* Ancient Ethiopian genome reveals extensive Eurasian admixture in Eastern Africa. *Science* **350**, 820–822 (2015).
47. Martiniano, R. *et al.* Genomic signals of migration and continuity in Britain before the Anglo-Saxons. *Nat. Commun.* **7**, 10326 (2016).
48. Olalde, I. *et al.* A common genetic origin for early farmers from Mediterranean Cardial and Central European LBK cultures. *Mol. Biol. Evol.* **32**, 3132–3142 (2015).
49. Rasmussen, M. *et al.* The genome of a Late Pleistocene human from a Clovis burial site in western Montana. *Nature* **506**, 225–229 (2014).
50. Rasmussen, M. *et al.* The ancestry and affiliations of Kennewick Man. *Nature* **523**, 455–458 (2015).
51. Schiffels, S. *et al.* Iron Age and Anglo-Saxon genomes from East England reveal British migration history. *Nat. Commun.* **7**, 10408 (2016).
52. Alexander, D. H., Novembre, J. & Lange, K. Fast model-based estimation of ancestry in unrelated individuals. *Genome Res.* **19**, 1655–1664 (2009).
53. Chang, C. C. *et al.* Second-generation PLINK: rising to the challenge of larger and richer datasets. *Gigascience* **4**, 7 (2015).
54. Purcell, S. *et al.* PLINK: a tool set for whole-genome association and population-based linkage analyses. *Am. J. Hum. Genet.* **81**, 559–575 (2007).
55. Busing, F. T. A., Meijer, E. & Leeden, R. Delete-m Jackknife for Unequal m. *Stat. Comput.* **9**, 3–8 (1999).
56. Moorjani, P. *et al.* Genetic evidence for recent population mixture in India. *Am. J. Hum. Genet.* **93**, 422–438 (2013).
57. Reich, D., Thangaraj, K., Patterson, N., Price, A. L. & Singh, L. Reconstructing Indian population history. *Nature* **461**, 489–494 (2009).

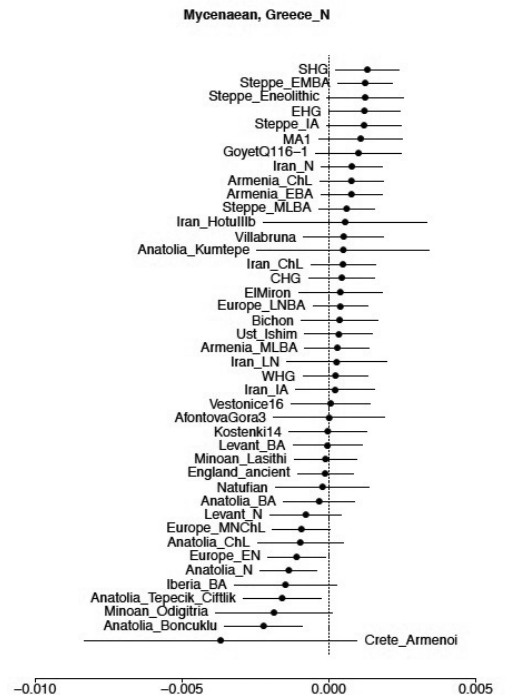


Extended Data Figure 1 | ADMIXTURE analysis. ADMIXTURE analysis (Methods) with $K = 2$ to $K = 17$ is shown. Three hundred and fifty-one ancient and 2,616 present-day individuals were used in this analysis; ancient samples and present-day Greeks are displayed. To avoid visual clutter of labels, individuals in populations with sample size ≤ 5 are shown with thicker lines.

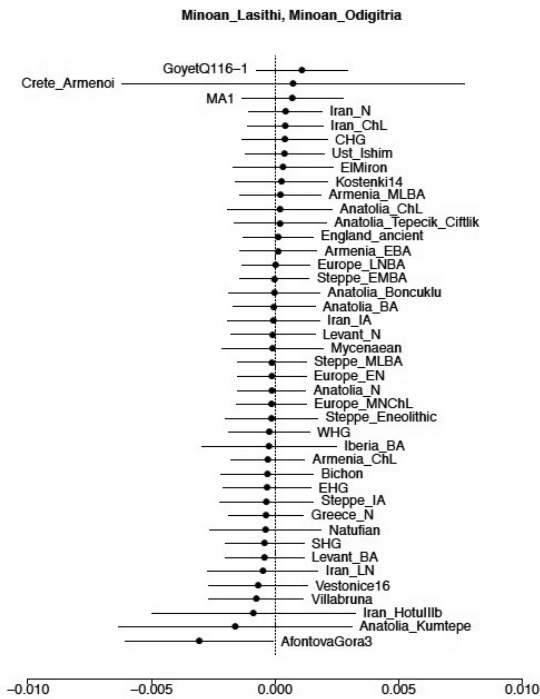
a



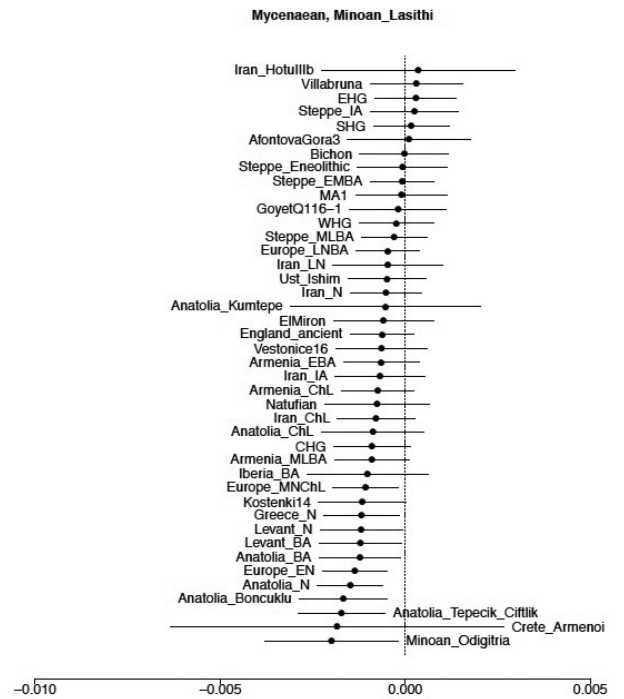
b



c

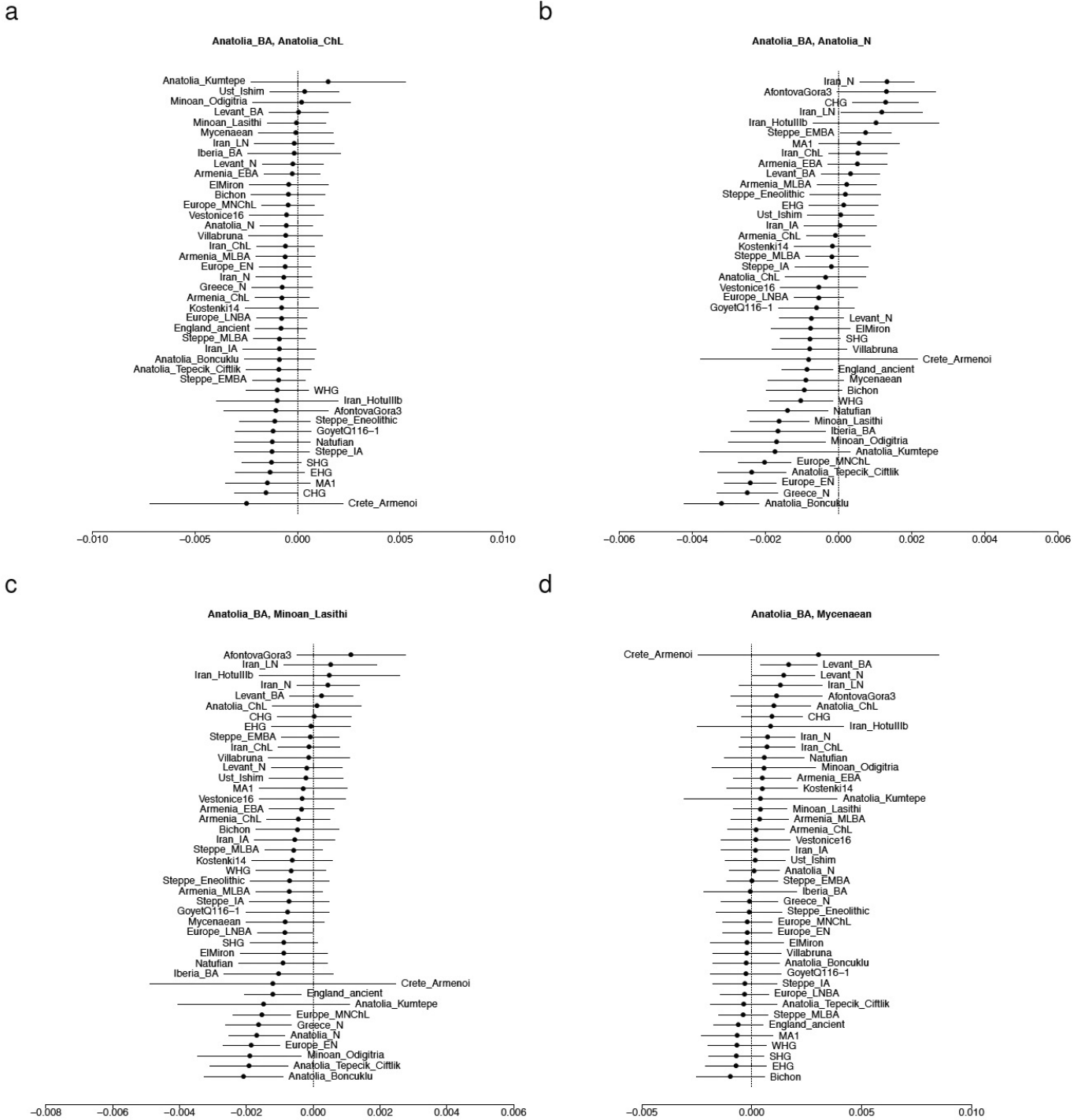


d



Extended Data Figure 2 | Symmetry testing of Aegean Bronze Age populations. The statistic $f_4(X, Y; \text{Test, Chimp})$ is shown with ± 3 standard errors. Each panel is titled with the pair X, Y . Populations are ordered according to the value of the statistic. Positive values indicate that Test shares more alleles with X than Y , and negative values that it shares more with Y than X . **a**, ‘Northern’ and ‘eastern’ populations share more alleles

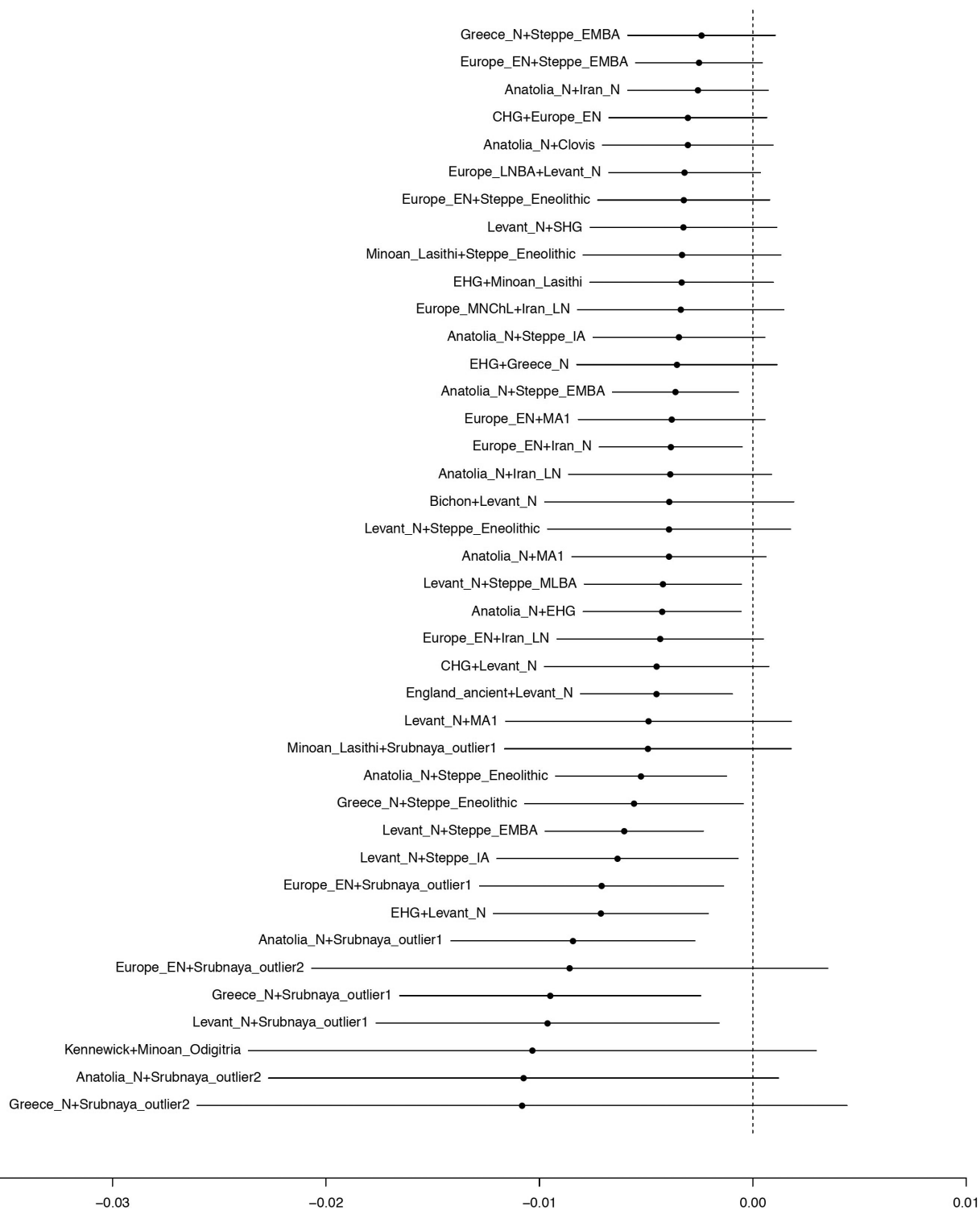
with Minoans than with Neolithic Greece. **b**, ‘Northern’ and ‘eastern’ populations share more alleles with Mycenaeans than with Neolithic Greece. **c**, Minoans from Lasithi and Moni Odigitria are symmetrically related to diverse populations. **d**, Neolithic populations from Anatolia, Europe, Greece, and the Levant share fewer alleles with Mycenaeans than with Minoans.



Extended Data Figure 3 | Symmetry testing of Anatolian Bronze Age populations. The statistic $f_4(X, Y; \text{Test}, \text{Chimp})$ is shown with ± 3 standard errors. Each panel is titled with the pair X, Y . Populations are ordered according to the value of the statistic. Positive values indicate that Test shares more alleles with X than Y , and negative values that it shares more with Y than X . **a**, European, Siberian, and Caucasus hunter-gatherers share fewer alleles with Bronze Age Anatolians from Harmanören Gündürle

than with a Chalcolithic Anatolian from Barçın. **b**, Bronze Age Anatolians differ from Neolithic ones in sharing more alleles with populations of Iran, the Caucasus, and the Steppe than with those of Europe. **c**, Bronze Age Anatolians differ from Minoans in sharing more alleles with populations from Neolithic Iran than Neolithic Anatolia and Europe. **d**, Bronze Age Anatolians differ from Mycenaean in sharing more alleles with Neolithic and Bronze Age populations of the Levant.

Mycenaean



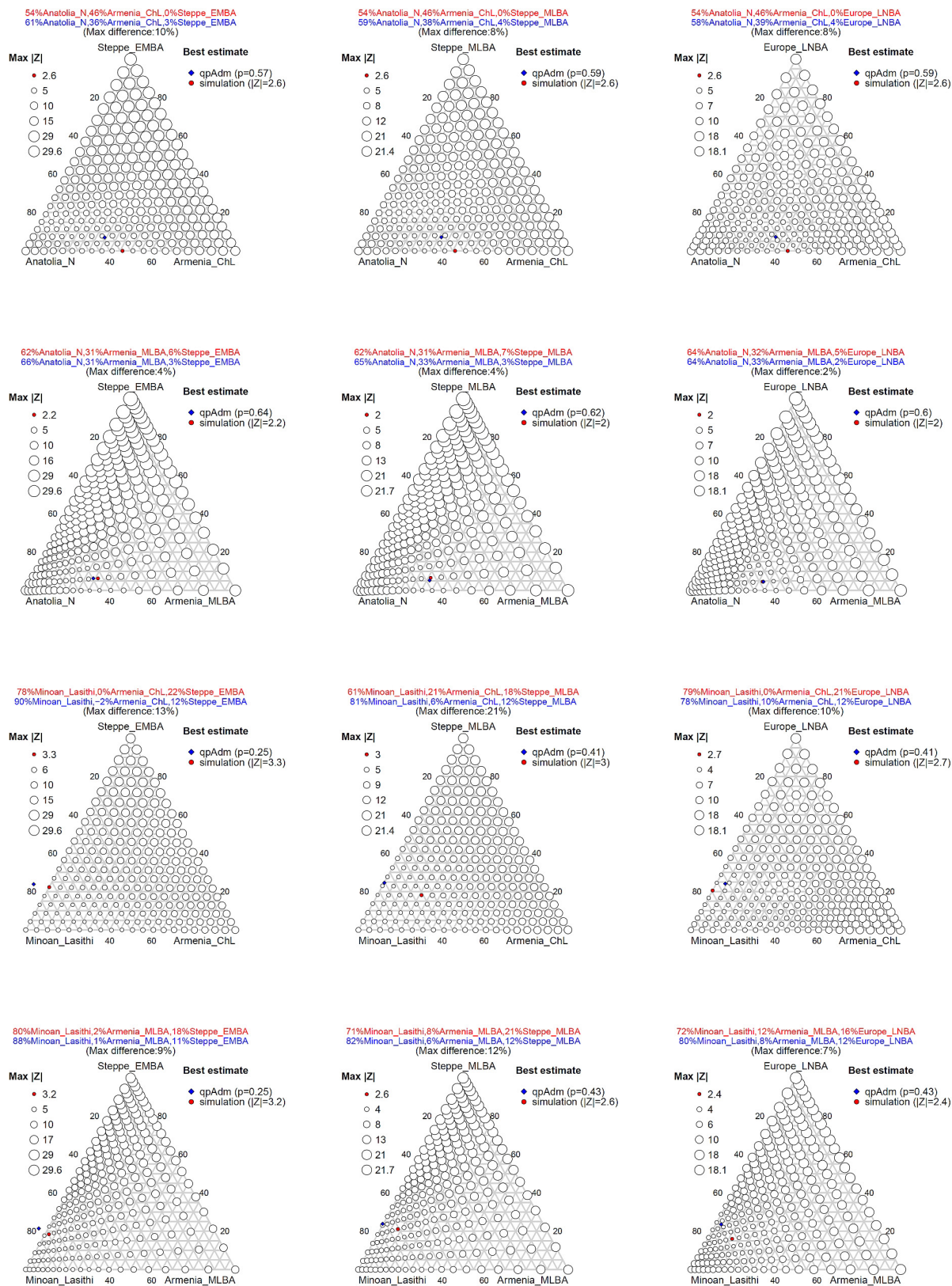
Extended Data Figure 4 | The f_3 -statistics of Mycenaean as a target with different pairs of reference populations. The value of the statistic $f_3(\text{Ref}_1, \text{Ref}_2; \text{Mycenaean})$ with ± 3 standard errors; only the population

pairs ($\text{Ref}_1, \text{Ref}_2$) for which the Z-score of the statistic is less than -2 are shown. Negative values indicate that the Mycenaean population is admixed from sources related to the two reference populations.



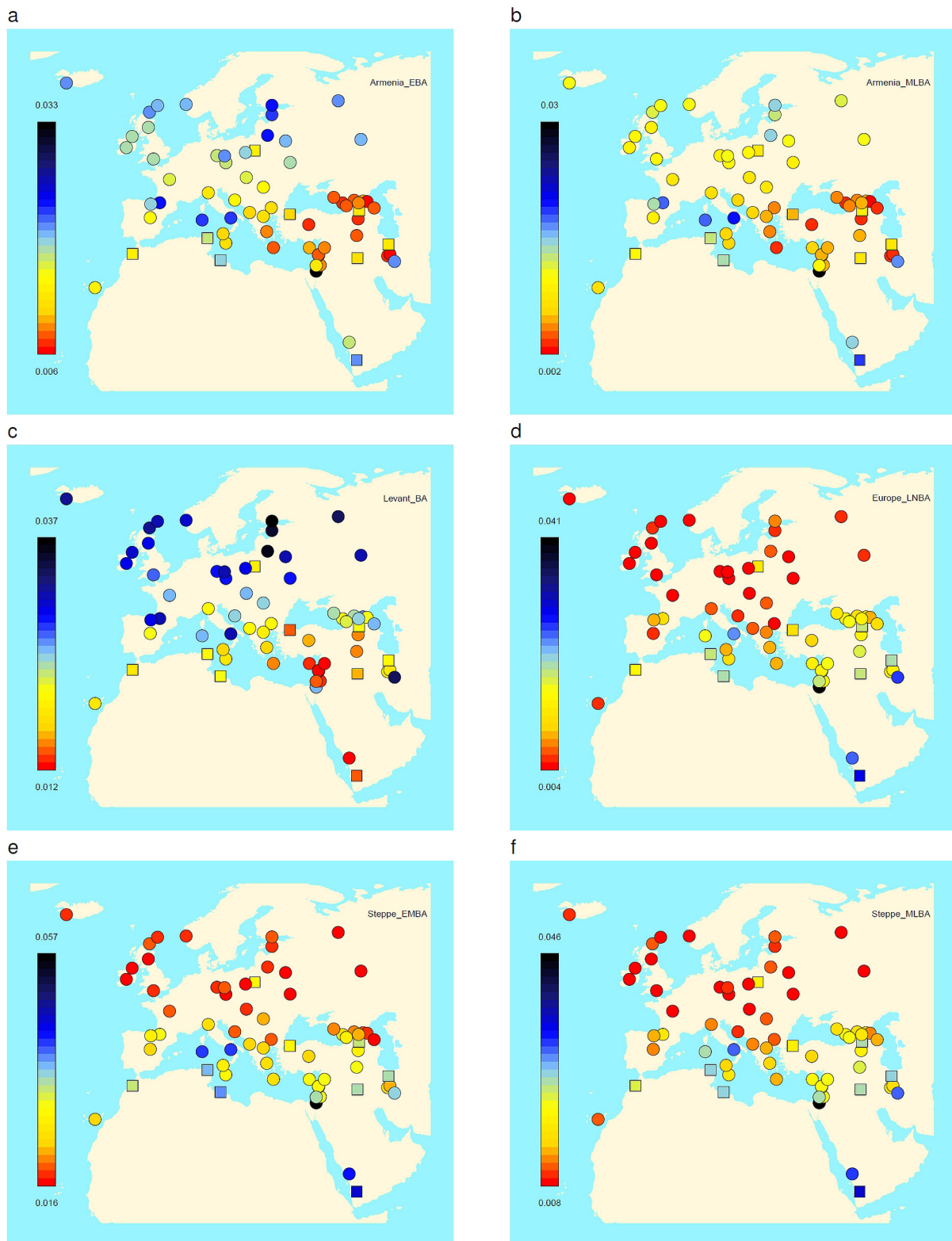
Extended Data Figure 5 | Correspondence of qpAdm estimates with PCA. As a way of validating qpAdm models of admixture for Mycenaean from three ancestral populations (Anatolia_N or Minoan_Lasithi), (Armenia_ChL or Armenia_MLBA), (Steppe_EMBA, Steppe_MLBA,

Europe_LNBA), representing substratum, 'eastern', and 'northern' ancestry, respectively (Supplementary Information section 2), we plot the qpAdm-predicted position in the PCA space of Fig. 1 versus the actual position of the Mycenaean population.



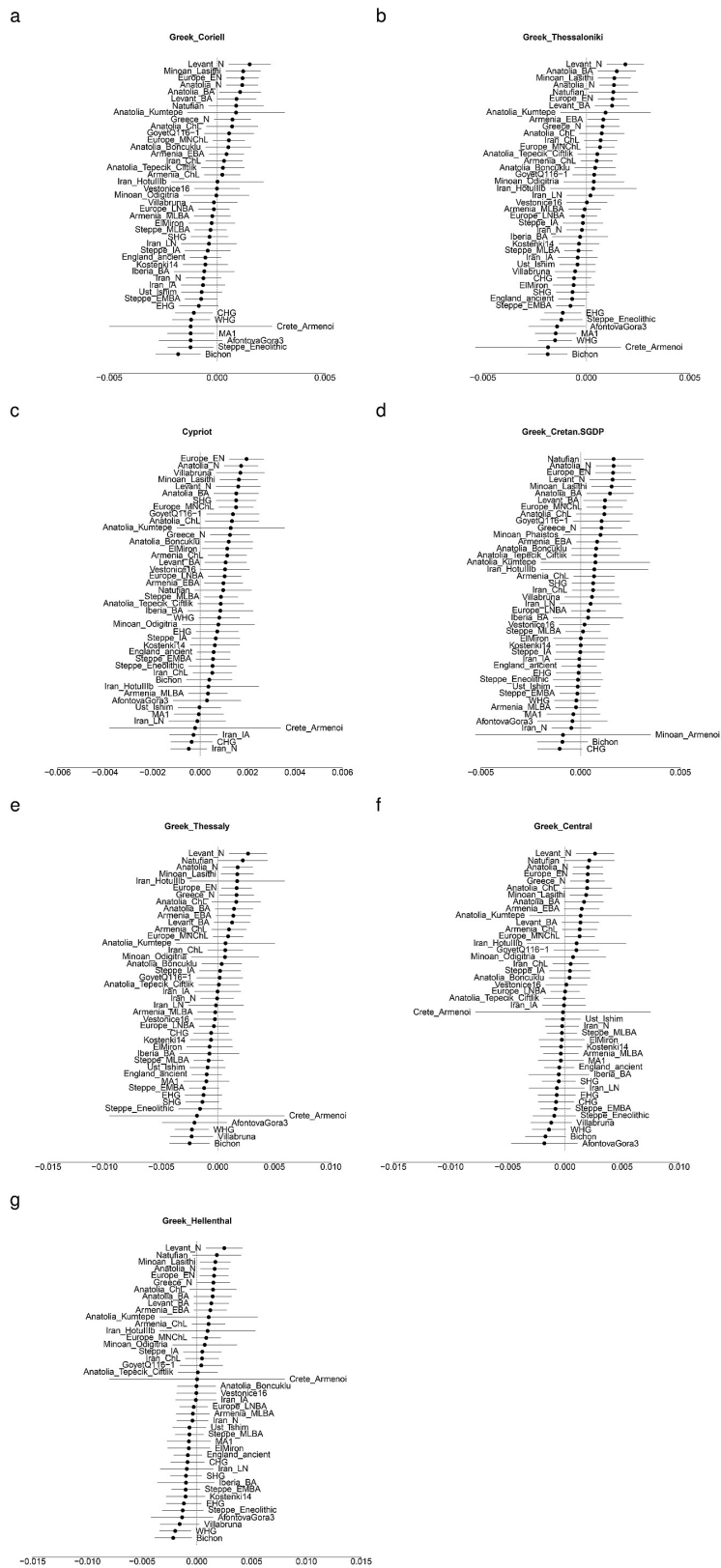
Extended Data Figure 6 | Comparison of Mycenaean and simulated admixed populations. We simulate admixed individuals with known ancestry from three ancestral populations (Anatolia_N or Minoan_Lasithi), (Armenia_ChL or Armenia_MLBA), (Steppe_EMBA, Steppe_MLBA, Europe_LNBA), representing substratum, ‘eastern’, and ‘northern’ ancestry, respectively (Methods and Supplementary Information section 2).

The maximum $|Z|$ -score of statistics $f_4(\text{Mycenaean, Simulated; Outgroup}_1, \text{Outgroup}_2)$ is plotted with circles of varying size (proportional to $\log(|Z|)$) for each assignment of ancestry proportions. The best estimate (red) corresponds to the proportions that minimize $|Z|$, and they are compared against the qpAdm estimate for the same ancestral sources (blue).



Extended Data Figure 7 | F_{ST} between Bronze Age and present-day West Eurasian populations. **a**, The population of Early Bronze Age Armenia⁴ shows an affinity to present-day populations from Armenia, Anatolia, the Caucasus, and Iran, as does **(b)** Middle/Late Bronze Age Armenia^{4,9}. **c**, The Bronze Age Levant⁴ has an affinity to Levantine and Arabian populations. **d**, Late Neolithic/Bronze Age Europeans^{1,6,9,43} most resemble present-day northern/central Europeans, as do **(e)** Early/Middle

Bronze Age steppe populations^{1,6,9}, who also resemble populations of the northeast Caucasus, while **(f)** Middle/Late Bronze Age steppe populations resemble central/northern Europeans^{1,9}. Jewish populations are plotted with a square to distinguish them from non-Jewish populations from the same geographical area. The plots for the newly reported populations of Mycenaeans, Minoans, and Bronze Age Anatolians are shown in Fig. 2.



Extended Data Figure 8 | Symmetry testing of Mycenaean with Modern Greek populations. The statistic f_4 (Mycenaean, Modern Greek; Test, Chimp) is shown with ± 3 standard errors. Modern Greeks share fewer alleles with Levantine/Anatolian/European Neolithic populations and with Minoans than Mycenaean, suggesting a dilution of Early Neolithic

ancestry since the Bronze Age. Human Origins genotype data: **a**, Greeks from the Coriell repository¹⁰; **b**, Greeks from Thessaloniki¹⁰; **c**, Cypriots¹⁰. Whole-genome data: **d**, Cretans⁴⁰. Illumina genotype data: **e**, Greeks from Thessaly⁴¹; **f**, Greeks from central Greece⁴¹; **g**, Greeks from the study in ref. 27.

Extended Data Table 1 | Information on ancient samples reported in this study

Individual_ID	Genotype_ID	Other_ID	Source	Date	Population_Label	Location	Country	Latitude	Longitude	Sex	Coverage	Autosomal_SNPs	mtDNA	Y-chromosome
I2937	I2937	A2197	1240K	5419±41 cal BC	Greece_N	Diros, Alepotrypa Cave	Greece	36.64	22.38	F	0.870	481848	K1a26	
I0071	I0071	Lasithi4	1240K	2000-1700 BCE	Minoan_Lasithi	Hagios Charalambos Cave, Lasithi, Crete	Greece	35.08	25.83	F	7.312	953157	U5a1	
I0070	I0070	Lasithi2	1240K	2000-1700 BCE	Minoan_Lasithi	Hagios Charalambos Cave, Lasithi, Crete	Greece	35.08	25.83	M	1.267	619767	H13a1	J2a1d
I0073	I0073	Lasithi7	1240K	2000-1700 BCE	Minoan_Lasithi	Hagios Charalambos Cave, Lasithi, Crete	Greece	35.08	25.83	M	1.481	643360	H	J2a1
I0074	I0074	Lasithi9	1240K	2000-1700 BCE	Minoan_Lasithi	Hagios Charalambos Cave, Lasithi, Crete	Greece	35.08	25.83	F	0.874	506434	H5	
I9005	I9005	Lasithi17	1240K	2000-1700 BCE	Minoan_Lasithi	Hagios Charalambos Cave, Lasithi, Crete	Greece	35.08	25.83	F	1.351	388859	H	
I9006	I9006	Salamis31	1240K	1411-1262 cal BCE (3087 ± 25 BP, DEM-2905)	Mycenaean	Agia Kyriaki, Salamis	Greece	37.97	23.50	F	1.387	361193	X2d	
I9123	I9123	S-EVA 1263 Armenoi 503	1240K	1370-1340 BCE	Crete_Armenoi	Armenoi, Crete	Greece	35.45	24.17	F	0.041	45158	U5a1	
I9127	I9127	12V t2	1240K	2900-1900 BCE	Minoan_Odigitria	Moni Odigitria, Heraklion, Crete	Greece	35.05	24.81	F	0.035	36475	J2b1a1	
I9128	I9128	13V t2	1240K	2900-1900 BCE	Minoan_Odigitria	Moni Odigitria, Heraklion, Crete	Greece	35.05	24.81	F	0.016	17081	I5	
I9129	I9129	14V t2	1240K	2900-1900 BCE	Minoan_Odigitria	Moni Odigitria, Heraklion, Crete	Greece	35.05	24.81	F	0.063	63986	H+163	
I9130	I9130	16V Tholos	1240K	2900-1900 BCE	Minoan_Odigitria	Moni Odigitria, Heraklion, Crete	Greece	35.05	24.81	M	0.086	92186	U3b3	G2a2b2
I9131	I9131	19V t2	1240K	2900-1900 BCE	Minoan_Odigitria	Moni Odigitria, Heraklion, Crete	Greece	35.05	24.81	F	0.095	96946	K1a2	
I9010	I9010	Galatas19	1240K	1700-1200 BCE	Mycenaean	Galatas Apatheia, Peloponnese	Greece	37.50	23.45	F	0.379	242265	X2	
I9033	I9033	Peristeria4	1240K	1416-1280 cal BCE (3084 ± 24 BP, DEM-2903)	Mycenaean	Peristeria Tryfilia, Peloponnese	Greece	36.92	21.70	F	0.439	248912	H	
I9041	I9041	Galatas4	1240K	1700-1200 BCE	Mycenaean	Galatas Apatheia, Peloponnese	Greece	37.50	23.45	M	1.558	417898	X2	J2a1
I2495	I2495	A4-1	1240K	2558-2295 calBCE (3925±35 BP, Poz-81111)	Anatolia_BA	Harmanören-Göndürle Höyük, Isparta	Turkey	37.92	30.71	M	1.981	637146	H	J1a
I2499	I2499	UC1	1240K	2836-2472 calBCE (4040±35 BP, Poz-82213)	Anatolia_BA	Harmanören-Göndürle Höyük, Isparta	Turkey	37.92	30.71	F	0.285	243348	K1a2	
I2683	I2683	G3-95	1240K	2500-1800 BCE	Anatolia_BA	Harmanören-Göndürle Höyük, Isparta	Turkey	37.92	30.71	F	3.695	749308	T2b	

Dates marked simply as BCE (Before Common Era) are based on the associated archaeology of the samples. Dates marked as calBCE are based on radiocarbon dating of the samples (Supplementary Information section 1).

Extended Data Table 2 | Phenotypic inference of ancient individuals

ID	Population	PBlueEye	PIntermediateEye	PBrownEye	PBlondHair	PBrownHair	PRedHair	PBlackHair	PLightHair	PDarkHair	Hair Color	Eye Color
I2495	Anatolia_BA	1.6 (4.4)	3.6 (3.9)	94.9 (8.3)	10.7 (6.1)	51.6 (6.4)	0.1 (0.1)	37.6 (9.3)	18.0 (11.7)	82.0 (11.7)	Brown	Brown
I2499	Anatolia_BA	16.6 (28.3)	7.4 (2.2)	76.0 (28.7)	2.2 (2.2)	64.7 (11.8)	2.0 (5.3)	31.1 (13.8)	12.9 (20.1)	87.1 (20.1)	Brown	Blue or Brown
I2683	Anatolia_BA	0.3 (0.9)	1.3 (1.7)	98.4 (2.6)	3.3 (2.5)	33.0 (4.6)	0.0 (0.0)	63.7 (7.0)	4.9 (4.5)	95.1 (4.5)	Black	Brown
I2937	Greece_N	0.3 (1.3)	2.2 (1.9)	97.5 (3.2)	3.6 (1.9)	33.9 (6.2)	0.1 (0.0)	62.4 (7.4)	6.7 (4.3)	93.3 (4.3)	Black	Brown
I0070	Minoan_Lasithi	0.4 (1.8)	2.2 (1.9)	97.4 (3.7)	30.4 (5.1)	66.4 (5.9)	3.2 (0.9)	0.0 (0.0)	100.0 (0.0)	0.0 (0.0)	Brown	Brown
I0071	Minoan_Lasithi	0.0 (0.0)	0.2 (0.0)	99.8 (0.0)	0.4 (0.0)	20.3 (0.0)	0.0 (0.0)	79.3 (0.0)	0.5 (0.0)	99.5 (0.0)	Black	Brown
I0073	Minoan_Lasithi	0.1 (0.7)	1.7 (1.4)	98.2 (2.2)	12.5 (3.4)	61.1 (1.2)	0.2 (0.1)	26.2 (2.7)	32.4 (8.8)	67.6 (8.8)	Brown	Brown
I0074	Minoan_Lasithi	0.0 (0.0)	1.3 (0.3)	98.7 (0.4)	9.3 (3.2)	54.8 (8.5)	0.1 (0.1)	35.8 (10.5)	18.8 (10.3)	81.2 (10.3)	Brown	Brown
I9005	Minoan_Lasithi	5.2 (0.0)	11.6 (0.0)	83.2 (0.0)	49.6 (1.4)	38.8 (1.2)	4.2 (0.5)	7.4 (0.7)	85.6 (1.7)	14.4 (1.7)	Blond or Brown	Brown
I9006	Mycenaean	0.0 (0.0)	1.1 (0.4)	98.9 (0.4)	8.7 (4.9)	59.9 (6.4)	1.8 (2.9)	29.6 (11.8)	25.7 (16.5)	74.3 (16.5)	Brown	Brown
I9033	Mycenaean	0.4 (1.0)	1.6 (1.9)	98.0 (3.0)	4.6 (3.9)	51.0 (6.3)	0.1 (0.5)	44.2 (9.8)	10.5 (13.2)	89.5 (13.2)	Brown	Brown
I9041	Mycenaean	1.4 (0.5)	5.3 (1.0)	93.3 (1.4)	7.8 (0.7)	63.2 (2.0)	0.2 (0.4)	28.7 (2.3)	21.2 (2.5)	78.8 (2.5)	Brown	Brown

We list the probability assignments for different phenotypes by HirisPlex²⁶ and an assessment of the phenotype. We generate 100 random replicates of the genotypes of each individual, listing the standard deviation in parentheses (Supplementary Information section 4).